

A Selective Chemosensor via Click Chemistry for Cu²⁺ and Hg²⁺ Ions in Organic Media

Sachin Kumar,^{1,2} Bajrang Lal,¹ Ram Kumar Tittal,^{1,*} Gurleen Singh,³ Jandeep Singh,³ Ghule Vikas D.,¹ Renu Sharma,² Jagjivan K. Sabane⁴

¹Department of Chemistry, National Institute of Technology, Kurukshetra, Haryana 136119, India

²School of Applied Sciences, Om Sterling Global University, Hisar, Haryana 125001, India

³School of Chemical Engineering and Physical Sciences, Lovely Professional University, Phagwara, Punjab 144411, India

⁴Division of Organic Chemistry, CSIR-National Chemical Laboratory, Dr. Homi Bhabha Road, Pune 411008, India

*Corresponding author: rktittaliitd@nitkkr.ac.in; Ph: +91-1744-233-542

Table of content:

S.No.	Contents	Page No.
1.	X-Ray Crystallography Experimental Section	S-3
2.	Table SI-1: Crystal data and structure refinement for 2.	S-3 to S-4
3.	Figure SI-1, Unit cell showing four molecular units in the asymmetric unit of compound 2	S-5
4.	Materials and methods: General information and materials, synthesis of 4-(di(prop-2-yn-1-yl) amino)-1,5- dimethyl-2-phenyl-1,2-dihydro-3H-pyrazol-3-one (1), synthesis of 2-azido-N-(1,5-dimethyl-3-oxo-2-phenyl-2,3-dihydro-1H-pyrazol-4-yl)acetamide (2)	S-5 to S-6
5.	General procedure for the synthesis of 1,4-disubstituted bis-1,2,3-triazole, APT	S-6 to S-7
6.	Figure SI 2-4, Physical data (FTIR, ¹ H-NMR, ¹³ C-NMR of 1)	S-7 to S-8
7.	Figure SI 5-8, Physical data (FTIR, ¹ H-NMR, ¹³ C-NMR, ESI-MS of 2)	S-9 to S-10
8.	Figure SI 9-13, Physical data (FTIR, ¹ H-NMR, ¹³ C-NMR, ESI MS, HRMS of probe APT)	S-11 to S-13
9.	Figure SI-14, Correlation plot of APT [(A _o -A _n)/A _n vs. Hg(II) concentration]	S-13
10.	Figure SI-15, Correlation plot of APT [(A _o -A _n)/A _n vs. Cu(II) concentration]	S-14
11.	Figure SI-16, Job Plot analysis of APT-metal complexation	S-14
12.	Figure SI-17, B-H plot for the complexation of APT with Hg(II)	S-15
13.	Figure SI-18, B-H plot for the complexation of APT with Cu(II)	S-15
14.	Figure SI-19, Absorption spectra of APT-Hg(II) complex solution showing the independence of absorption intensity of time	S-16
15.	Figure SI-20, Absorption spectra of APT-Cu(II) complex solution showing the independence of absorption intensity of time	S-16
16.	Figure SI-21, The absorption spectra of Hg(II)-bound APT solution, after being subjected to a temperature range of 20-50°C	S-17
17.	Figure SI-22, The absorption spectra of Cu(II)-bound APT solution, after being subjected to a temperature range of 20-50°C	S-17
18.	Figure SI-23, Optimized Structures of (a) Alkyne, 1 and (b)	S-18

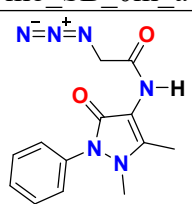
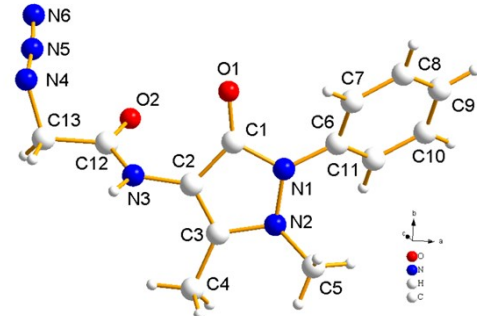
Azide, **2**

19.	Figure SI-24, Optimized Structure of APT	S-18
20.	Figure SI-25, Optimized Structures of APT.Cu ²⁺ and APT.Hg ²⁺	S-18
21.	Table SI-2 Calculated FMOs, energy gap in eV at the B3LYP/6-311G(d,p) and B3LYP/LanL2DZ level of theory.	S-19
22.	Figure SI-26, Highest occupied and lowest unoccupied molecular orbitals (HOMO and LUMO) distribution at the ground state of molecules 1, 2, APT, APT.Cu ²⁺ and APT.Hg ²⁺ complex	S-19 to S-20
23.	Figure SI-27, Contour plots of the frontier orbitals of the complex APT.Hg²⁺ .	S-21
24.	References	S-22

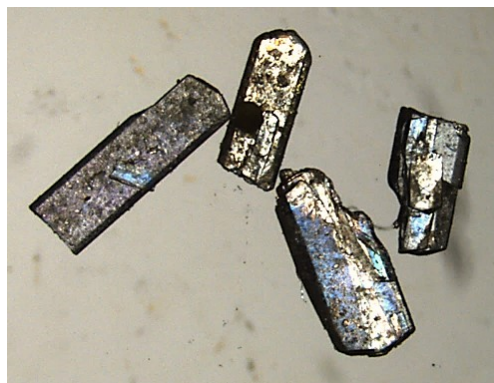
X-Ray Crystallography Experimental Section:

A block-shaped clear whiteish color single crystals were carefully picked under a polarizing microscope and pasted to an excellent fine glass fiber with the help of cyanoacrylate (superglue) adhesive. The single-crystal X-ray diffraction data were collected with Bruker APEX-II CCD diffractometer with monochromatic Mo $K\alpha$ radiation ($\lambda = 0.71073 \text{ \AA}$) at 100(2) K by using ω and ϕ scan. The X-ray generator was operated at 50 kV and 20 mA. The data were reduced by using APEX3, the SAINT V8.40A (Bruker, 2019) program and was used for diffraction profiles integration. The structure was solved and refined by the full-matrix least square method on F^2 using the SHELXL 2018/3 & SHELXT 2018/2 program^{1,2} respectively, present in the Olex2 package of programs (version 1.3.0)³. All the hydrogen positions were initially located in the different Fourier maps. For the final refinement, the hydrogen atoms were placed in geometrically ideal positions and refined in the riding mode. The final refinement comprised the atomic positions of all the atoms, isotropic thermal parameters for all the hydrogen atoms, and anisotropic thermal parameters for all the non-hydrogen atoms. Please refer to the following **Table SI-1** for a detailed explanation of the crystal structure solution and final refinements for the structures. The crystallographic data for compound **2** can be found in CCDC No: **2254070** free of charge from The Cambridge Crystallographic Data Centre (CCDC) via www.ccdc.cam.ac.uk/data_request/cif.

Table SI-1 Crystal data and structure refinement for **2**.

Compound	2
Identification code	mo_SB_0m_a
Molecular Structure	
Crystal Structure (CCDC: 2254070)	

Crystal Image



Empirical formula	C₁₃H₁₄N₆O₂
Formula weight	286.30
Temperature/K	100(2)
Crystal system	'Monoclinic'
Space group	'P2₁/n'
a/Å	13.3072(7)
b/Å	6.9369(3)
c/Å	15.2738(9)
α/°	90
β/°	106.507(2)
γ/°	90
Volume/Å ³	1351.82(12)
Z	4
ρ _{calc} /cm ³	1.407
μ/mm ⁻¹	0.101
Radiation	MoKα (λ = 0.71073)
2θ range for data collection/°	4.794 to 68.222
Reflections collected	92555
Independent reflections	5503 [R _{int} = 0.0871, R _{sigma} = 0.0458]
Data/restraints/parameters	5503/0/192
Final R indexes [I ≥ 2σ (I)]	R ₁ = 0.0447, wR ₂ = 0.1027
Final R indexes [all data]	R ₁ = 0.0751, wR ₂ = 0.1143
Largest diff. peak/hole / e Å ⁻³	0.41/-0.32

The X-ray single-crystal structure investigation revealed that compound **2** was shaped in a monoclinic crystal system. Compound **2** crystallizes in monoclinic cells with space group *P2₁/n*. The resultant structure of compound **2** contains four molecular units in the asymmetric unit and is represented in **Figure SI-1**. In the crystal structure, one can find four molecular structures anti-parallel to each other similar to the mirror image with respect to the 1,2,3-triazole unit in the middle.

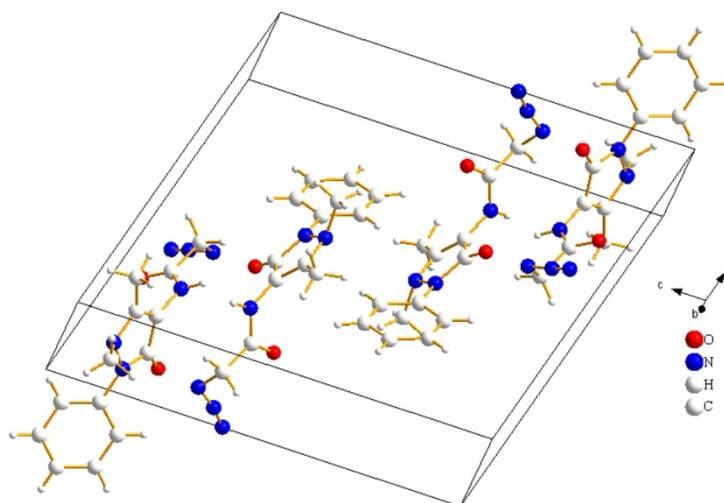


Figure SI-1. Unit cell showing four molecular units in the asymmetric unit of compound **2**.

Materials and methods

General information and materials:

All chemicals used for the reaction were purchased from sources available commercially and were used as it is without any further purification. 4-aminoantipyrine was purchased from (Loba Chemie), propargyl bromide (Sigma Aldrich), potassium carbonate (Loba Chemie), chloroacetyl chloride (Loba Chemie) and sodium azide (Loba Chemie). Chlorides of various metal ions such as Ba(II), Zn(II), Ca(II), Cd(II), Cu(II), Hg(II), Mg(II), Pb(II), Ni(II), Co(II), Mn(II) and Cr(III) were purchased from Loba Chemie. Solvents were brought from Finar, S.D. Fine and Loba Chemie. $^1\text{H-NMR}$ and $^{13}\text{-NMR}$ were recorded using Jeol ECZ 400S and Bruker Avance Neo 500 MHz instrument with TMS (tetramethylsilane) as standard internal reference. Mass spectra were recorded using XEVO G2-XS QTOF spectrometer. FTIR was obtained from Shimadzu spectrophotometer. Metal ion sensing studies were done using a SHIMADZU UV-1900 spectrometer with quartz cuvette.

Synthesis of 4-(di(prop-2-yn-1-yl) amino)-1,5- dimethyl-2-phenyl-1,2-dihydro-3H-pyrazol-3-one, (1):

Bis-alkyne was prepared by following known method⁴. 4-aminoantipyrine (1 equiv.) was dissolved in 8-10 mL of DMF in a 50 mL oven-dried Rb flask (round bottom flask). Potassium carbonate (5 equiv. of 4-aminoantipyrine) was added to the above solution and the reaction mixture was stirred for 20 min. After that propargyl bromide (2.2 equiv.) was added dropwise with constant stirring and the reaction mixture was continuously stirred for 18 hrs. at room temperature. The progress of reaction was monitored with TLC. After completion,

the workup was done in ice-cold water to get precipitates. The solid appeared were then filtered and washed with water to remove DMF. Further, recrystallization of precipitates was performed in ACN (acetonitrile) to get crystalline product.

Brown solid, Yield: 95%, m.p. 123-125°C. FTIR (ν_{\max} cm^{-1}): 3269, 3205, 2995, 2933, 2837, 2113, 1651, 1498, 1288 cm^{-1} ; ^1H NMR (400 MHz, CDCl_3) δ 7.48-7.26 (m, 5H), 3.96 (d, $J=4\text{Hz}$, 4H), 3.05 (s, 3H), 2.30 (s, 3H), 2.23 (t, $J=4\text{Hz}$, 2H); ^{13}C NMR (101 MHz, CDCl_3) δ 163.40(C), 153.83(C), 135.14(C), 129.19(CH), 126.45(CH), 123.69(CH), 118.69(C), 80.74(C), 77.16(CH), 72.26(CH), 42.84(CH_2), 36.44(CH_3), 10.83(CH_3).

Synthesis of 2-azido-N-(1,5-dimethyl-3-oxo-2-phenyl-2,3-dihydro-1H-pyrazol-4-yl)acetamide, (2):

The synthesis of chloroacetyl chloride derivative of 4-aminoantioyrine was performed by following reported procedure⁵ with some further modifications. 1 mmol of 4-aminoantipyrene was dissolved in 10 mL DCM in a 100 mL Rb flask. Potassium carbonate (1.5 equiv.) was added to the above Rb flask. The reaction mixture was allowed to stir at ice bath. A solution of chloroacetyl chloride (1.2 equiv.) was added dropwise to the reaction mixture and after addition, the reaction was refluxed for 10-12 hrs. On completion of reaction monitored by TLC, the workup was done by filtration and then evaporation of filtrate on rota evaporator. Solid appeared was washed with plenty of water and after drying used as it is for azidation. The solid obtained was dissolved in minimum amount of ACN (Acetonitrile). 1.5 equiv. sodium azide was added to the above reaction mixture. On completion of reaction, the mixture was filtered and then filtrate was evaporated on rota evaporator. Solid appeared was washed with water and dried under vacuum.

Pale yellow solid, Yield: 90%, m.p. 158-160°C, FTIR (ν_{\max} cm^{-1}): 3238, 3207, 3024, 2958, 2096, 1693, 1490, 1307 cm^{-1} . ^1H NMR (400 MHz, CDCl_3) δ 9.36 (s, H), 7.32-7.49 (m, 5H), 3.88 (s, 2H), 3.11 (s, 3H), 2.22 (s, 3H); ^{13}C NMR (101 MHz, CDCl_3) δ 167.42 (C), 162.13 (C), 150.51 (C), 134.53 (C), 129.86 (CH), 128.07 (CH), 125.35 (CH), 107.72 (C), 52.36 (CH_2), 36.09 (CH_3), 12.61 (CH_3). ESI-MS $[\text{M}+\text{H}]^+$: m/z cal. for $\text{C}_{43}\text{H}_{45}\text{N}_{15}\text{O}_5\text{H}^+$ is 287.125, found 287.147.

Synthesis of 1,4-disubstituted bis-1,2,3-triazole, APT:

The synthesis of 1,2,3-triazole derivative was performed by following standard reported procedure. 1 mmol of alkyne **1** dissolved in 8 mL EtOH in a 100 mL round bottom flask. To

this 2.2 mmol of organic azide **2** was added by dissolving in minimum amount of EtOH. To the above reaction mixture copper sulfate and sodium ascorbate (10 and 20 mol %, respectively) was added by dissolving in water (1 mL, each). The reaction was completed in less than 30 minutes. On completion, it was quenched with water, off-white solid appeared was washed with water and dried under vacuum.

Off-white solid, Yield: 89 %, m.p. 240-241°C. FTIR (ν_{\max} cm^{-1}): 3265, 3188, 3030, 2922, 2854, 1701, 1309, 759 cm^{-1} . ^1H NMR (400 MHz, CDCl_3) δ 9.63 (s, 2H), 7.92 (s, 2H), 7.27-7.50 (m, 15H), 5.28(s, 4H), 4.27 (s, 4H), 3.04 (s, 6H), 2.80 (s, 3H), 2.11 (s, 6H), 1.75 (s, 3H); ^{13}C NMR (101 MHz, CDCl_3) δ 165.06 (C), 161.41 (C), 151.94 (C), 134.88 (C), 129.13 (C), 128.91 (CH), 126.39 (CH), 125.76 (CH), 125.15 (CH), 123.64 (CH), 123.18 (C), 106.57 (C), 51.43 (CH_2), 48.27 (CH_2), 35.90 (CH_3), 11.23 (CH_3), 9.75 (CH_3). ESI-MS $[\text{M}+\text{H}]^+$: m/z cal. for $\text{C}_{43}\text{H}_{45}\text{N}_{15}\text{O}_5\text{H}^+$ is 852.3802, found 852.3802.

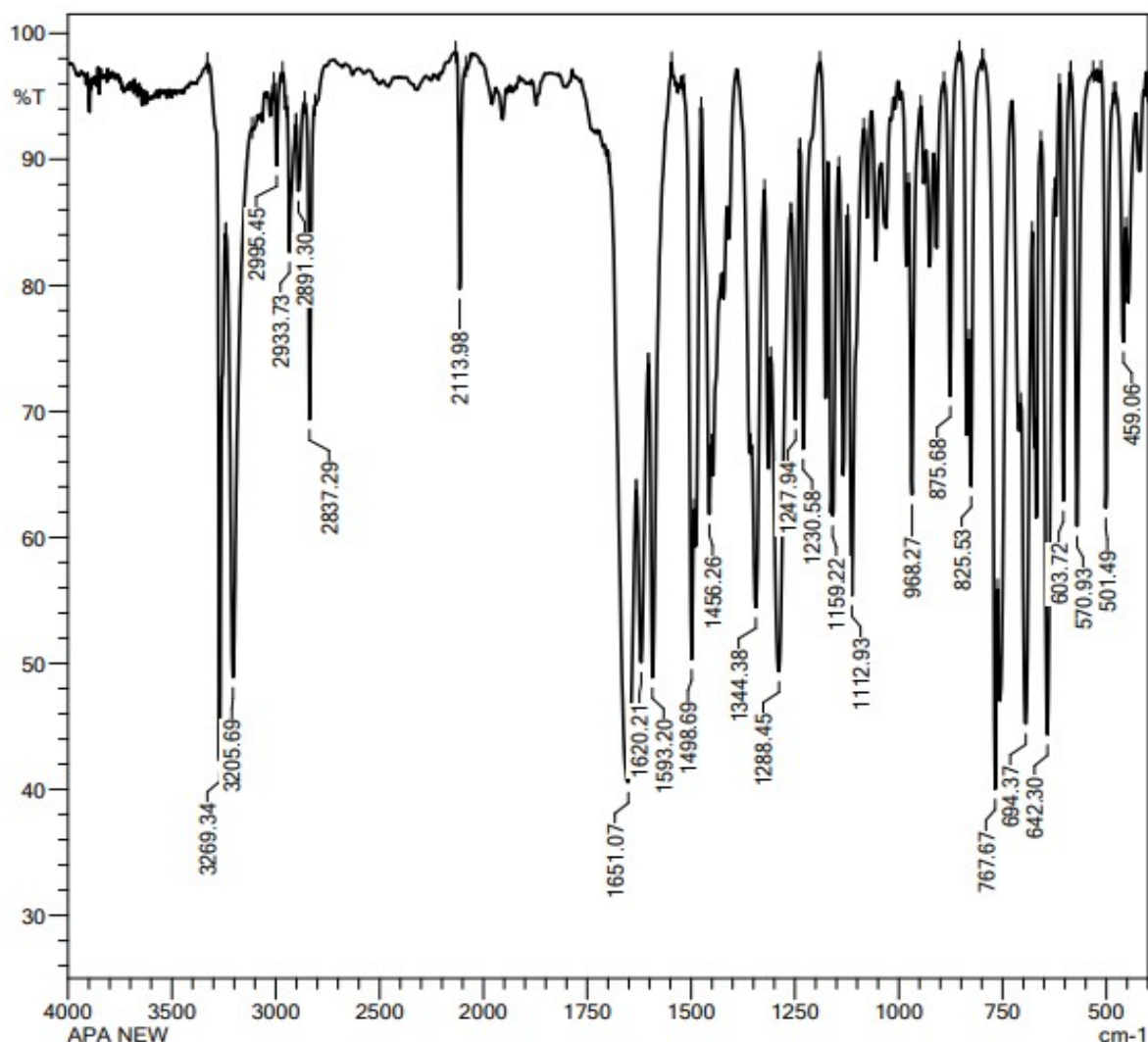


Figure SI-2 FTIR bis-alkyne, 1

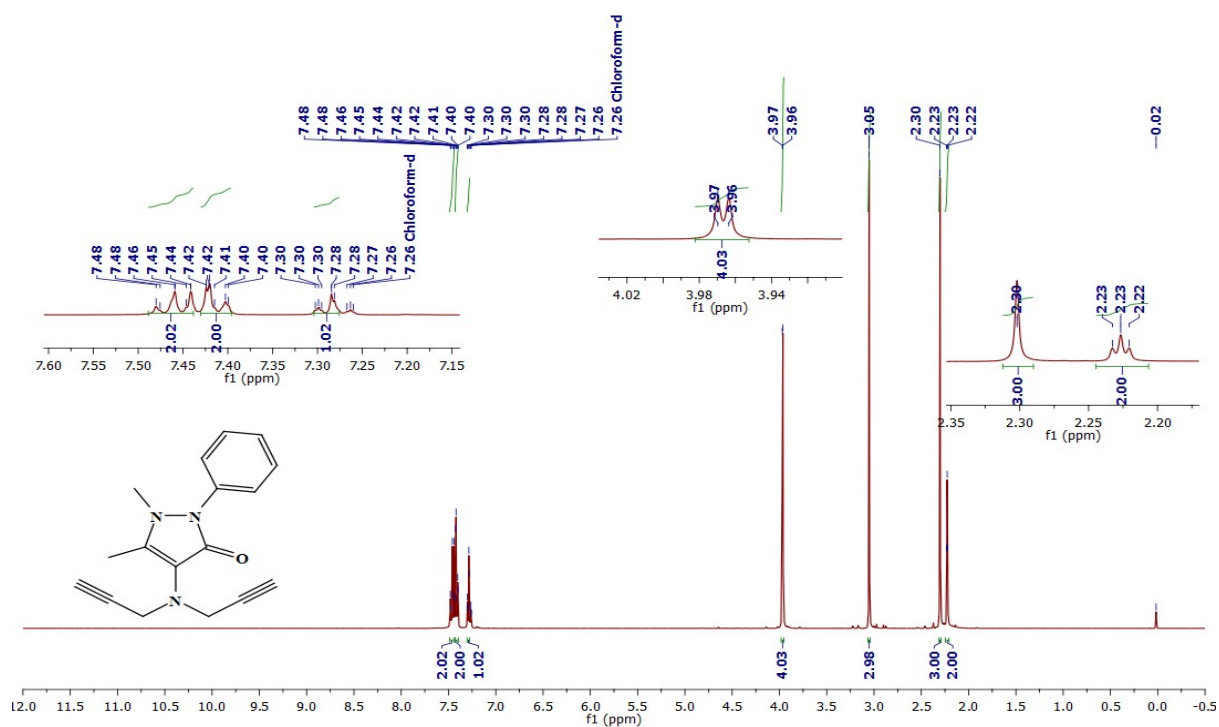


Figure SI-3 $^1\text{H-NMR}$ bis-alkyne, **1**

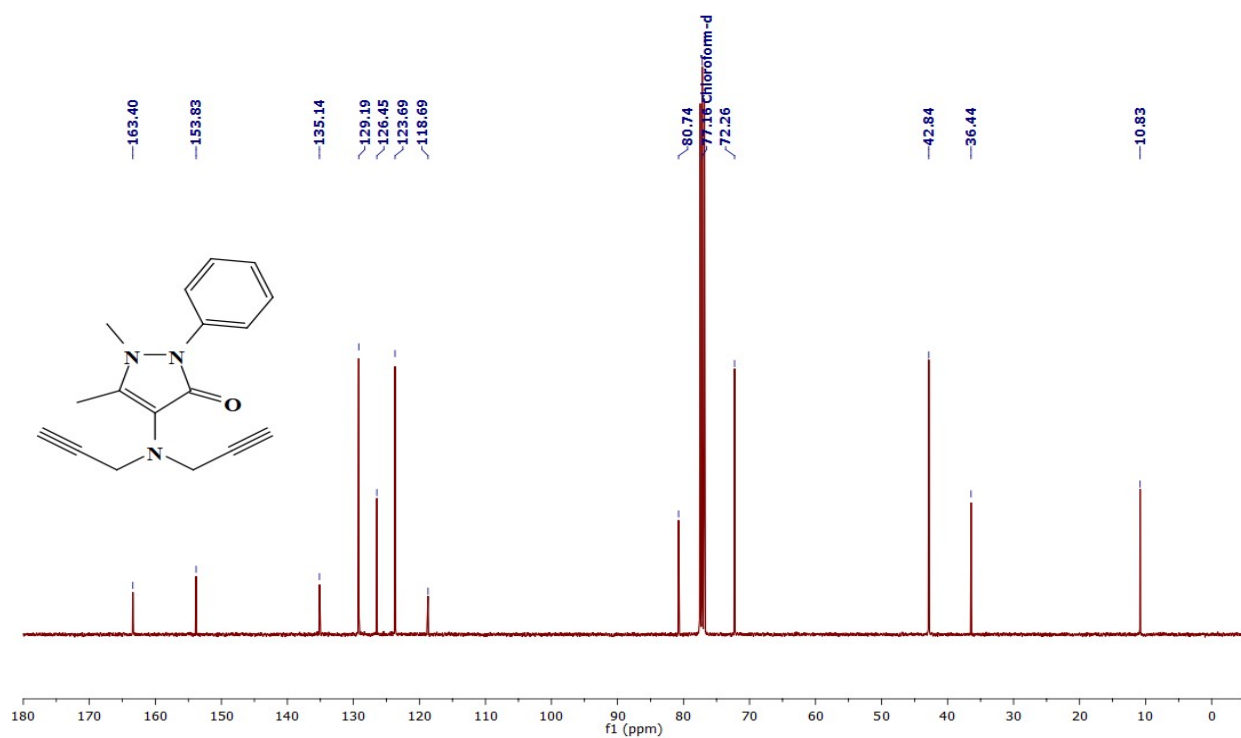


Figure SI-4 $^{13}\text{C-NMR}$ Spectra of bis-alkyne, **1**

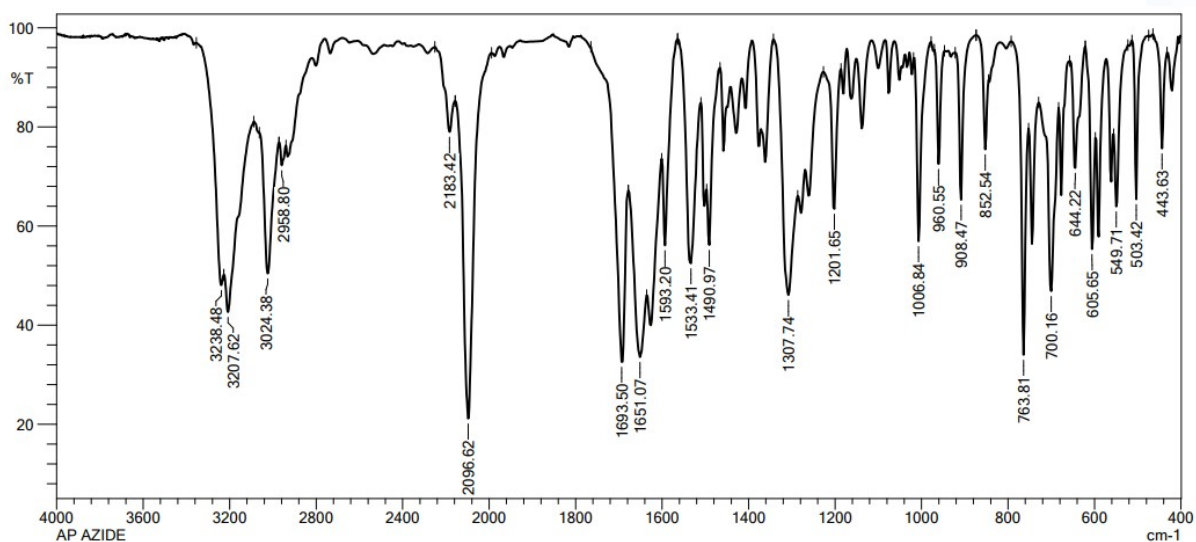


Figure SI-5. IR spectra of organic azide, 2

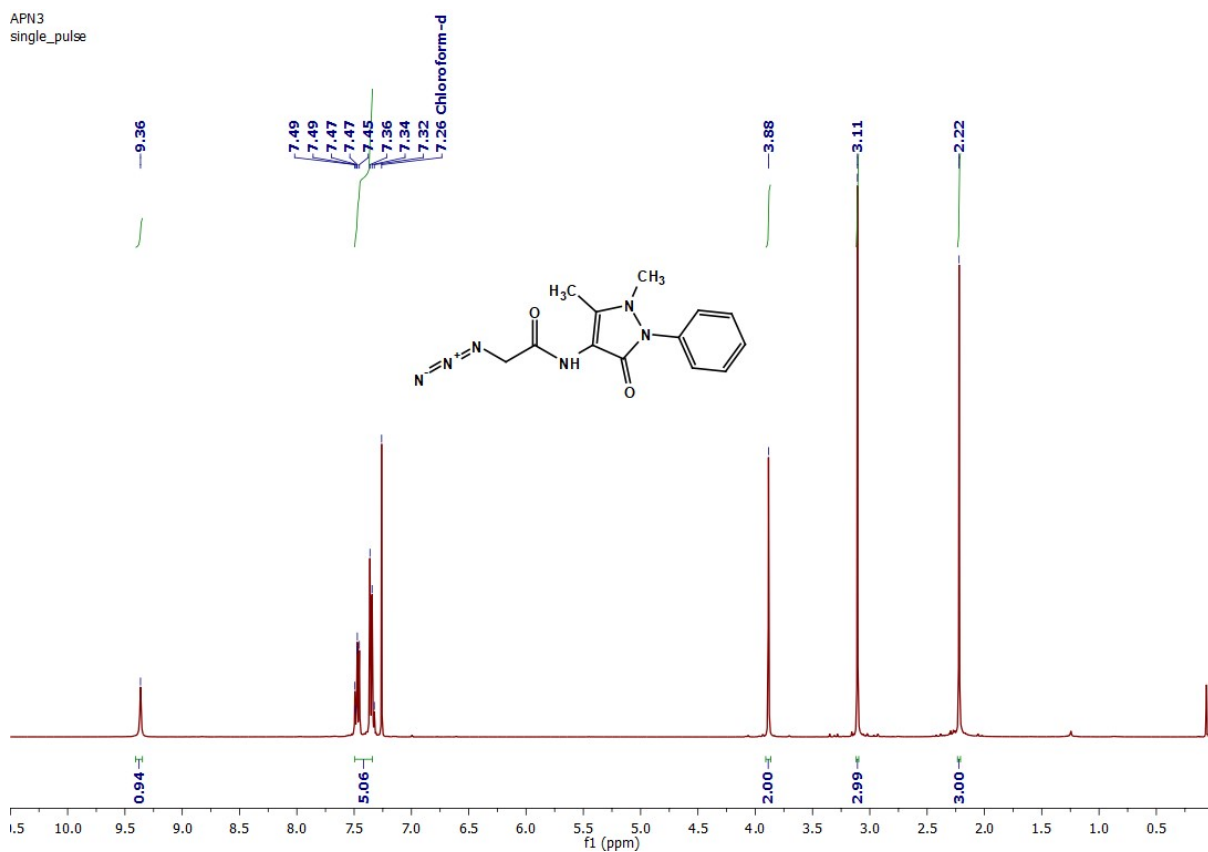


Figure SI-6. ¹H NMR spectra of organic azide, 2

APN3
single pulse decoupled gated NOE

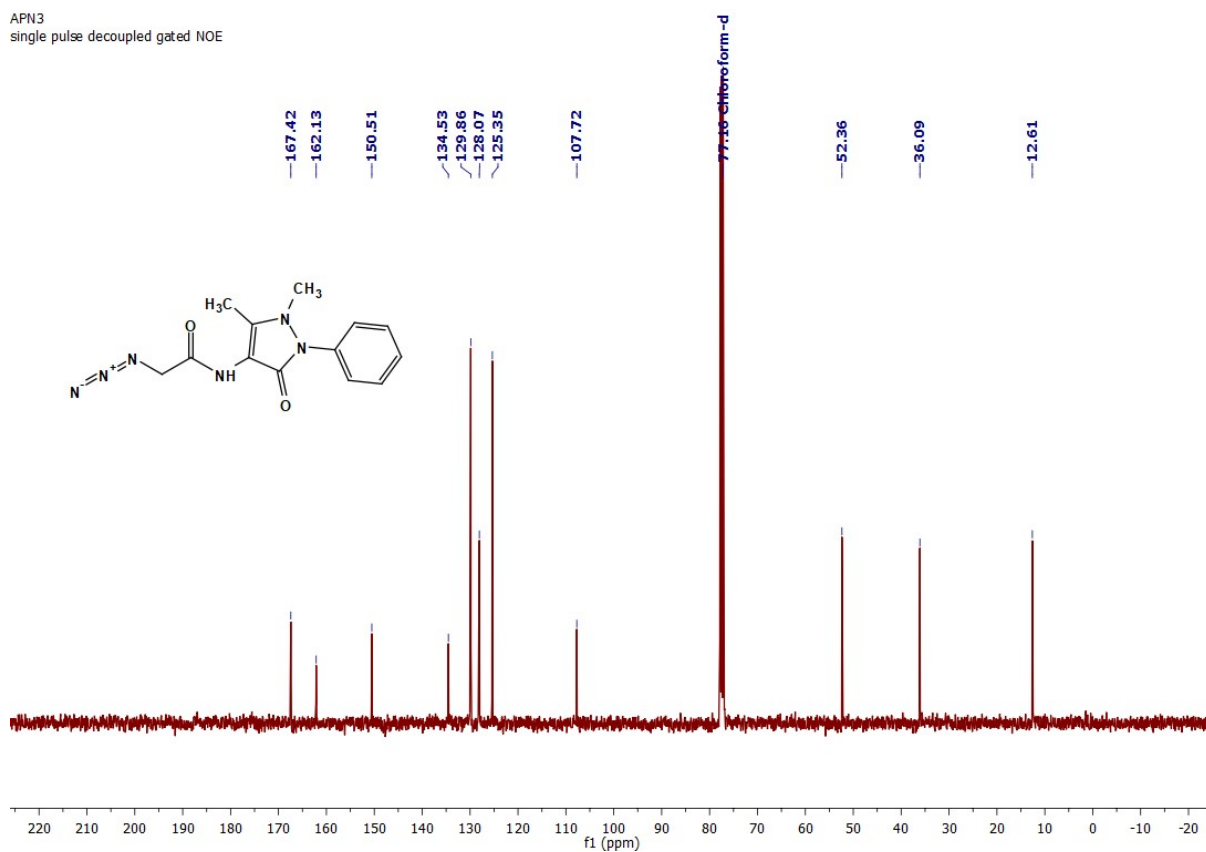


Figure SI-7. ¹³C NMR spectra of organic azide, 2

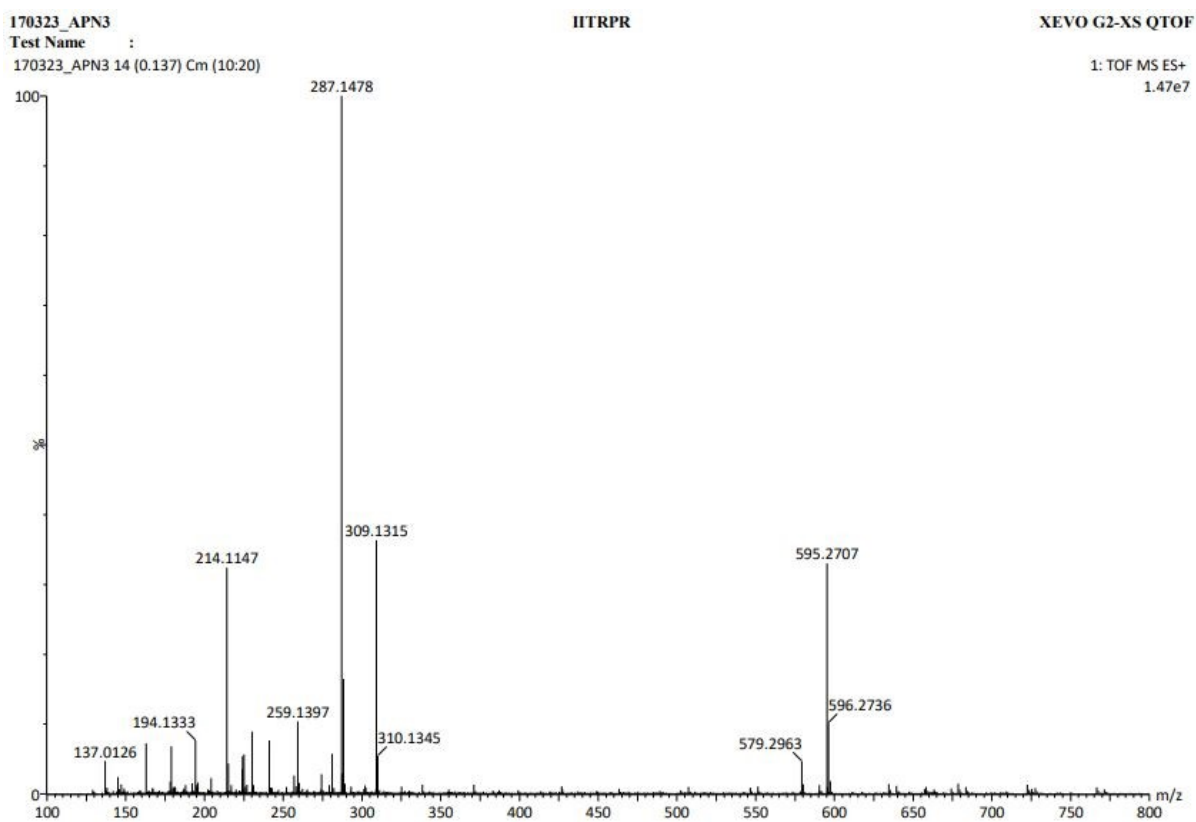


Figure SI-8. ESI-MS spectra of organic azide, 2

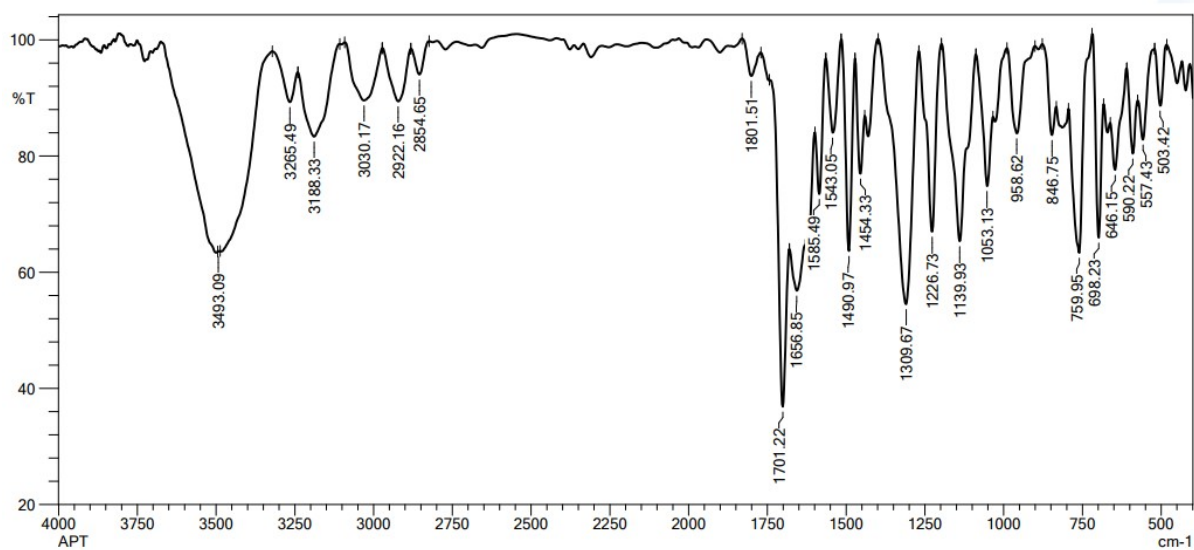


Figure SI-9. IR spectra of APT

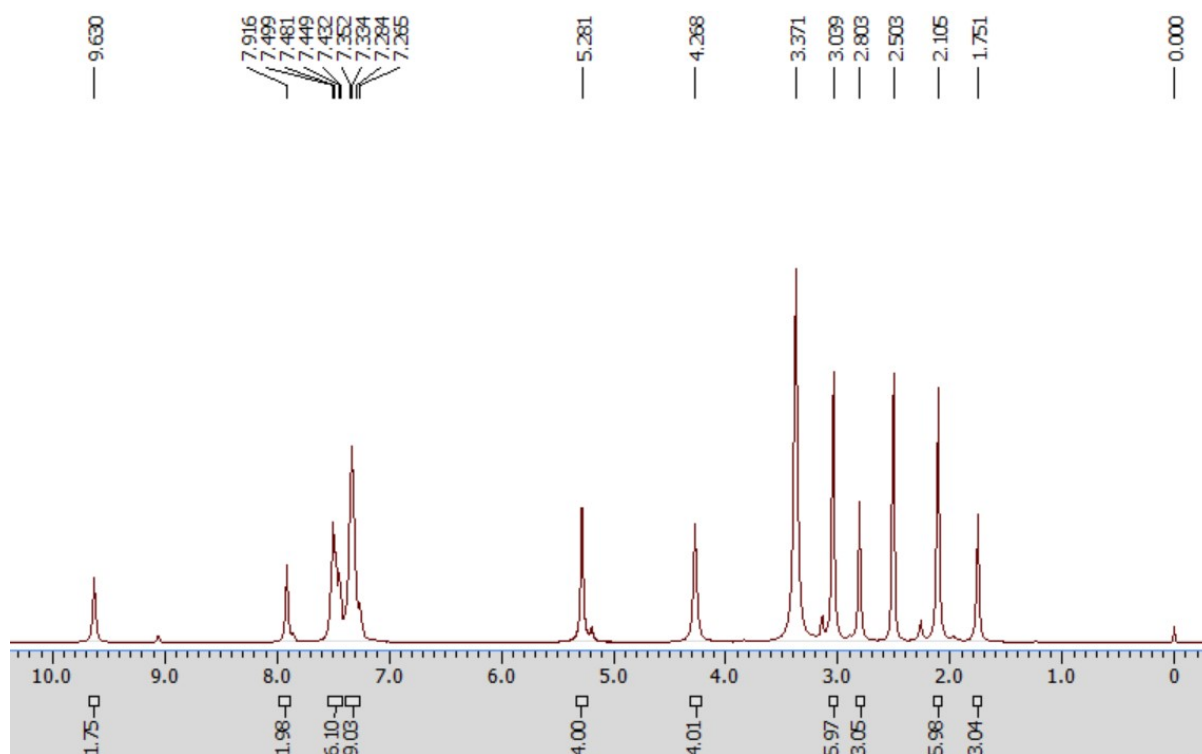


Figure SI-10. ¹H NMR spectra of APT

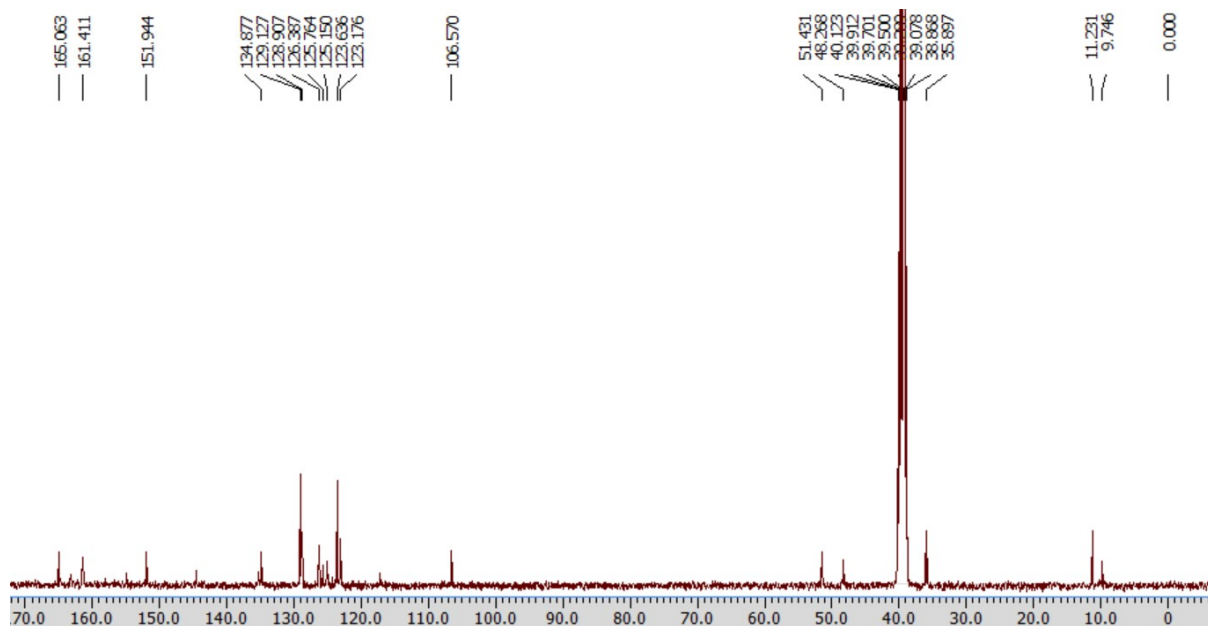


Figure SI-11. ^{13}C NMR spectra of APT

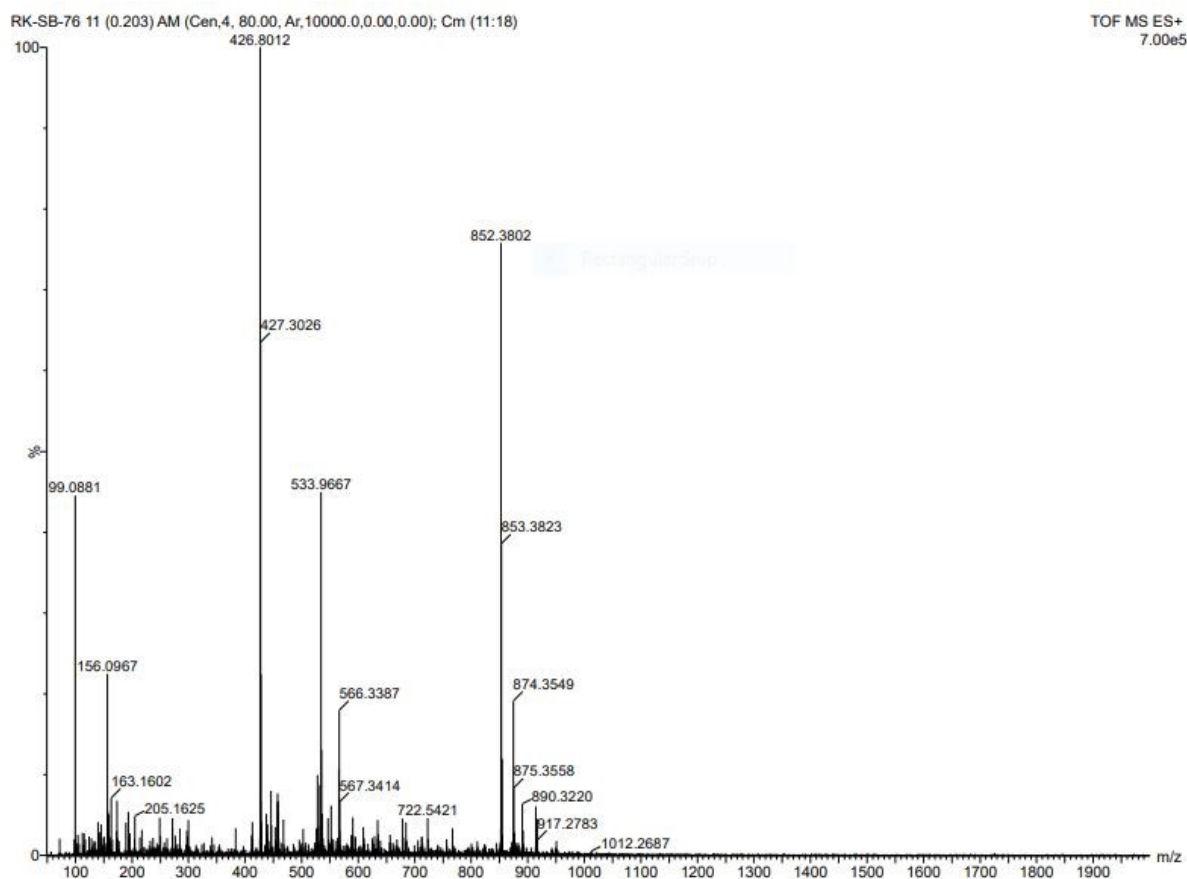


Figure SI-12. ESI-MS spectra of APT

Elements Used:

C: 1-43 H: 1-60 N: 1-15 O: 1-5

080623_SB_76 26 (0.285)

Test Name

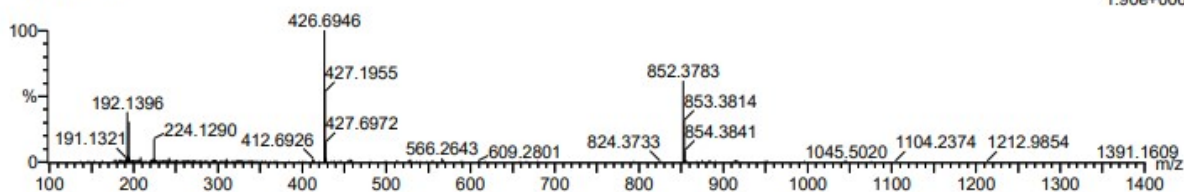
1: TOF MS ES+

IITRPR

XEVO G2-XS QTOF

080623_SB_76

1.90e+006



Minimum: -1.5
Maximum: 5.0 20.0 50.0

Mass	Calc. Mass	mDa	PPM	DBE	i-FIT	Norm	Conf (%)	Formula
852.3783	852.3806	-2.3	-2.7	28.5	585.0	n/a	n/a	C43 H46 N15 O5

Figure SI-13. HRMS spectra of APT

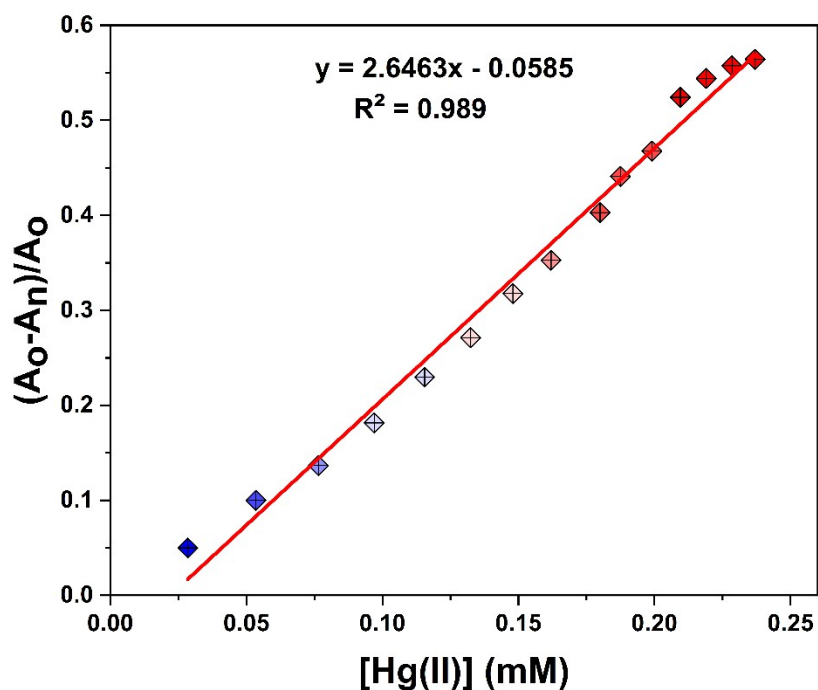


Figure SI-14. Correlation plot of APT [(A_o-A_n)/A_n vs. Hg(II) concentration]

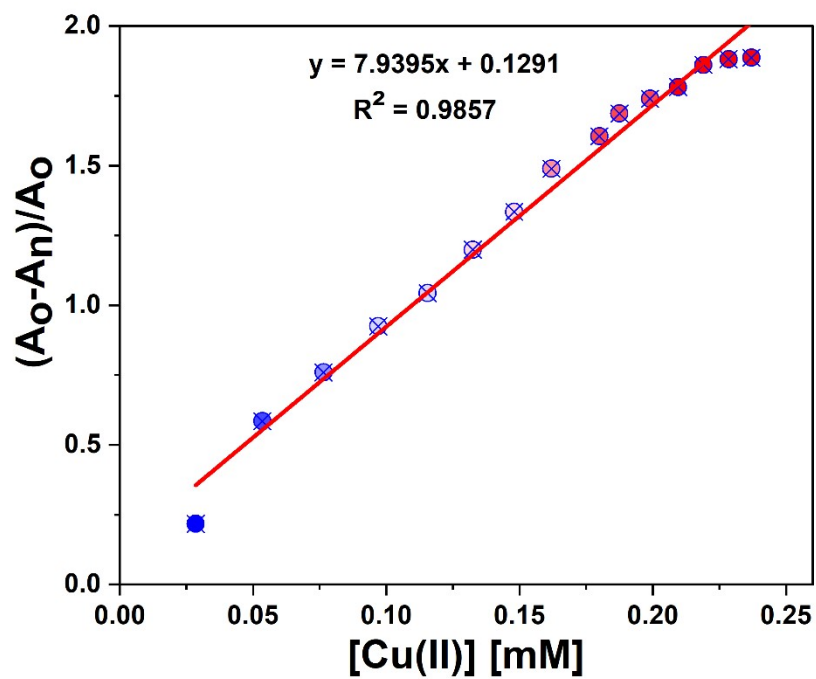


Figure SI-15. Correlation plot of APT $[(A_0 - A_n)/A_0]$ vs. Cu(II) concentration

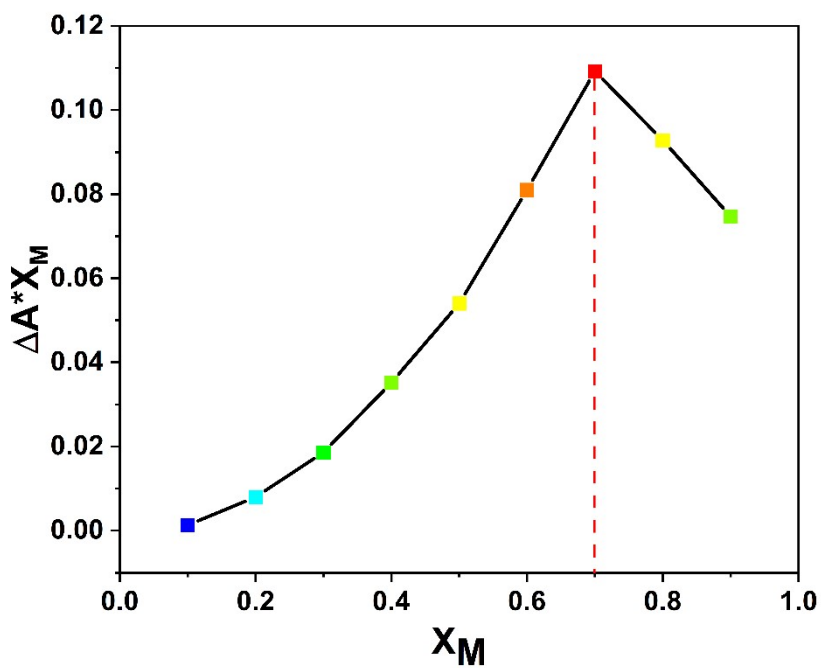


Figure SI-16. Job Plot analysis of APT-metal complexation

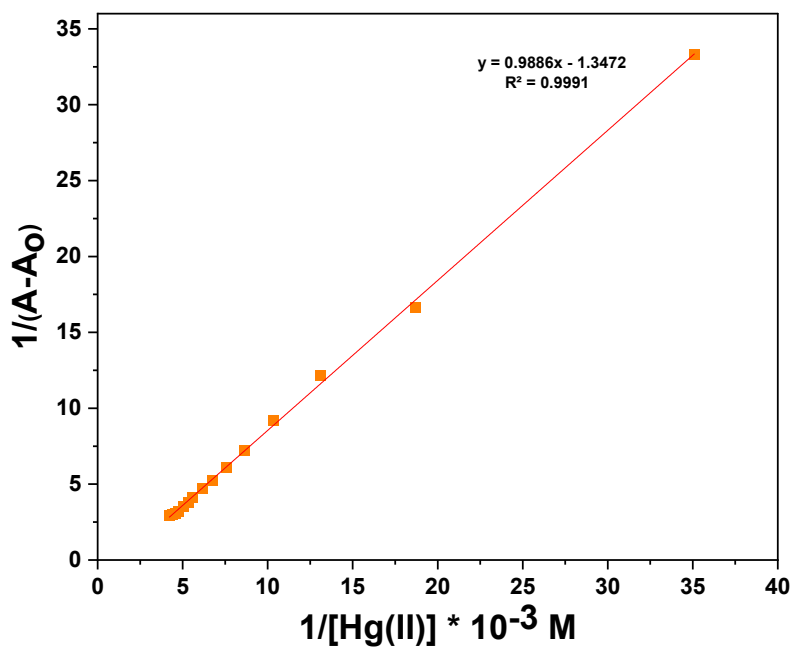


Figure SI-17. B-H plot for the complexation of APT with Hg(II)

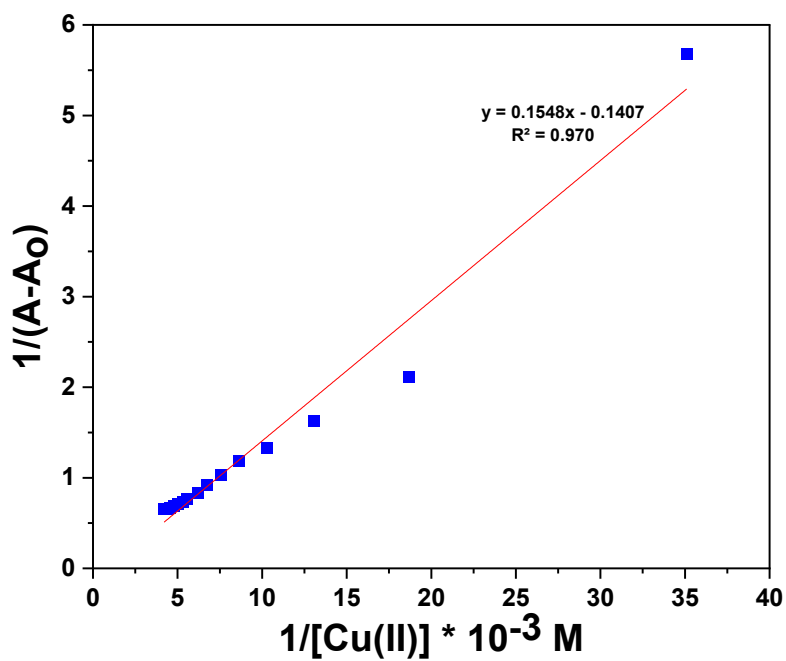


Figure SI-18. B-H plot for the complexation of APT with Cu(II)

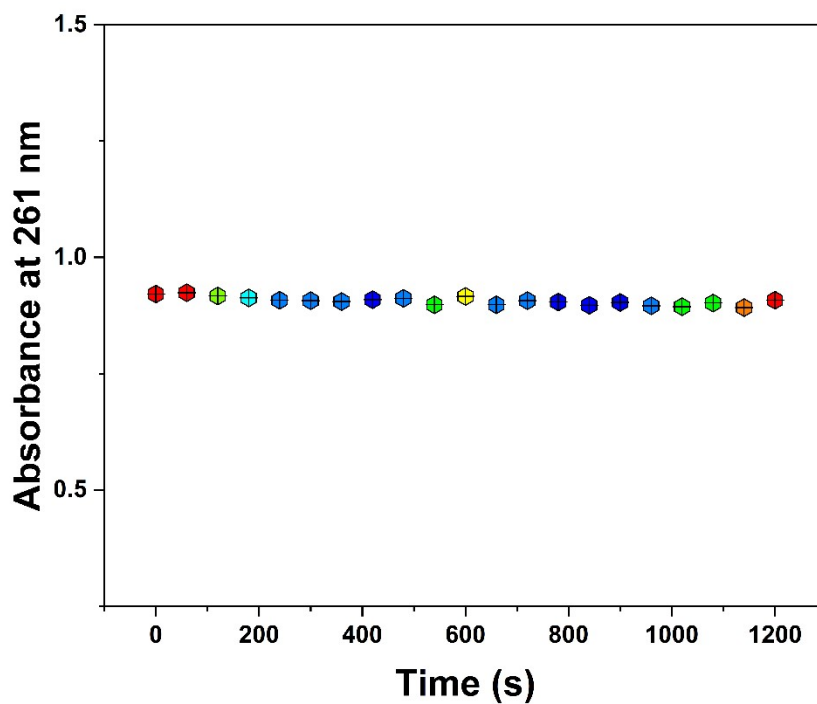


Figure SI-19. Absorption spectra of APT-Hg(II) complex solution showing the independence of absorption intensity of time

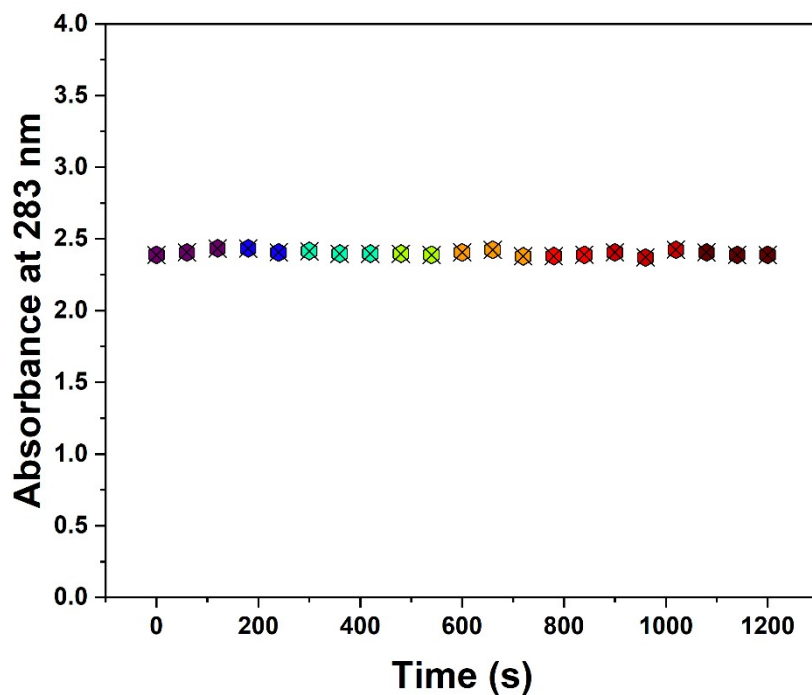


Figure SI-20. Absorption spectra of APT-Cu(II) complex solution showing the independence of absorption intensity of time

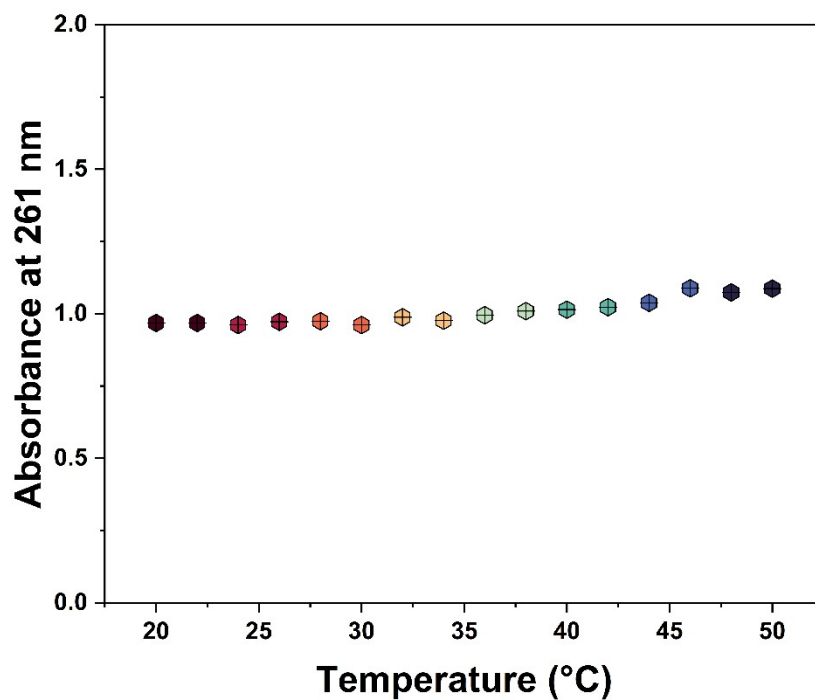


Figure SI-21. The absorption spectra of Hg(II)-bound APT solution, after being subjected to a temperature range of 20-50°C

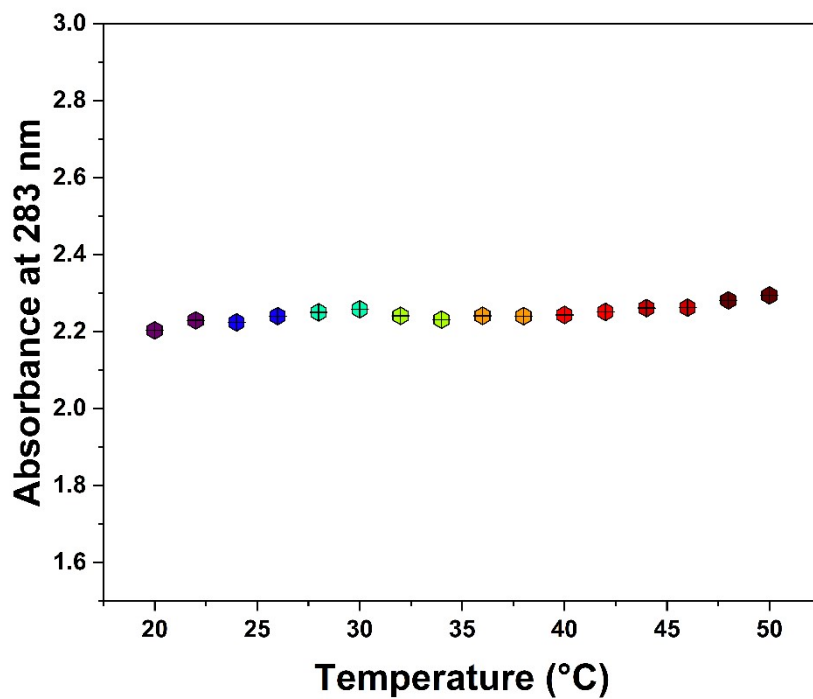


Figure SI-22. The absorption spectra of Cu(II)-bound APT solution, after being subjected to a temperature range of 20-50°C

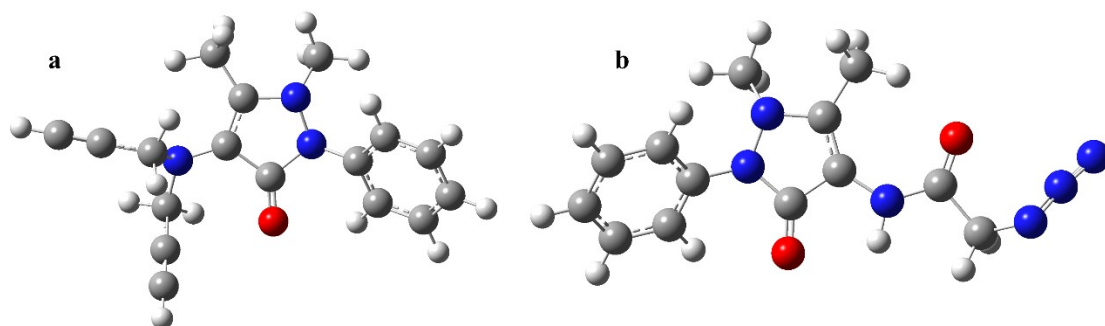


Figure SI-23. Optimized Structures of (a) Alkyne, **1** and (b) Azide, **2**

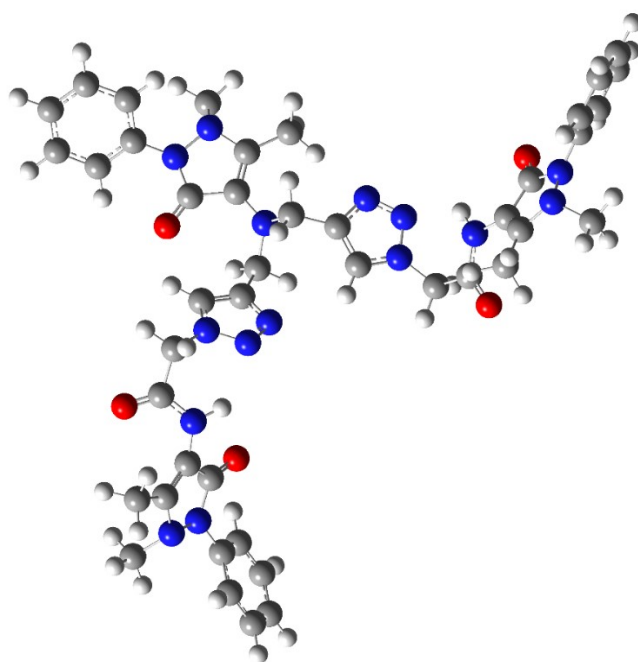


Figure SI-24. Optimized Structure of APT

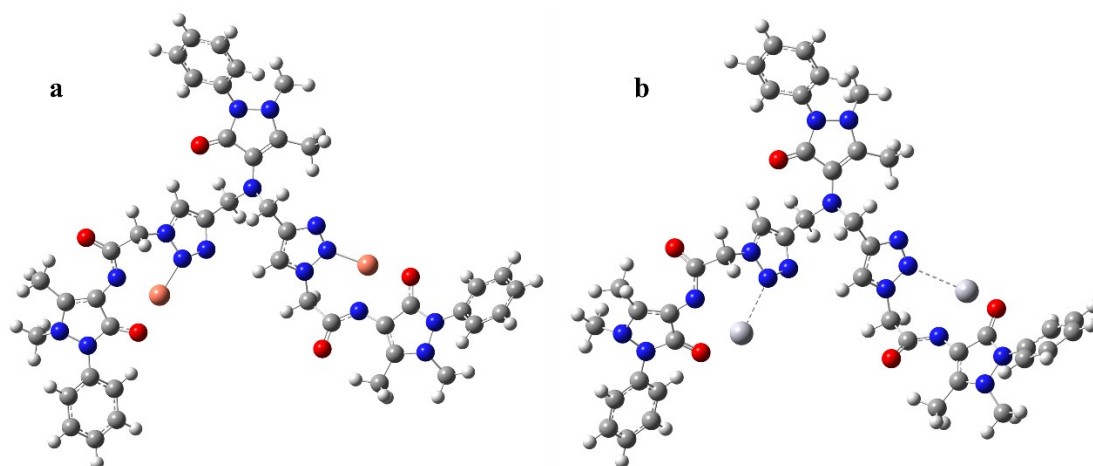
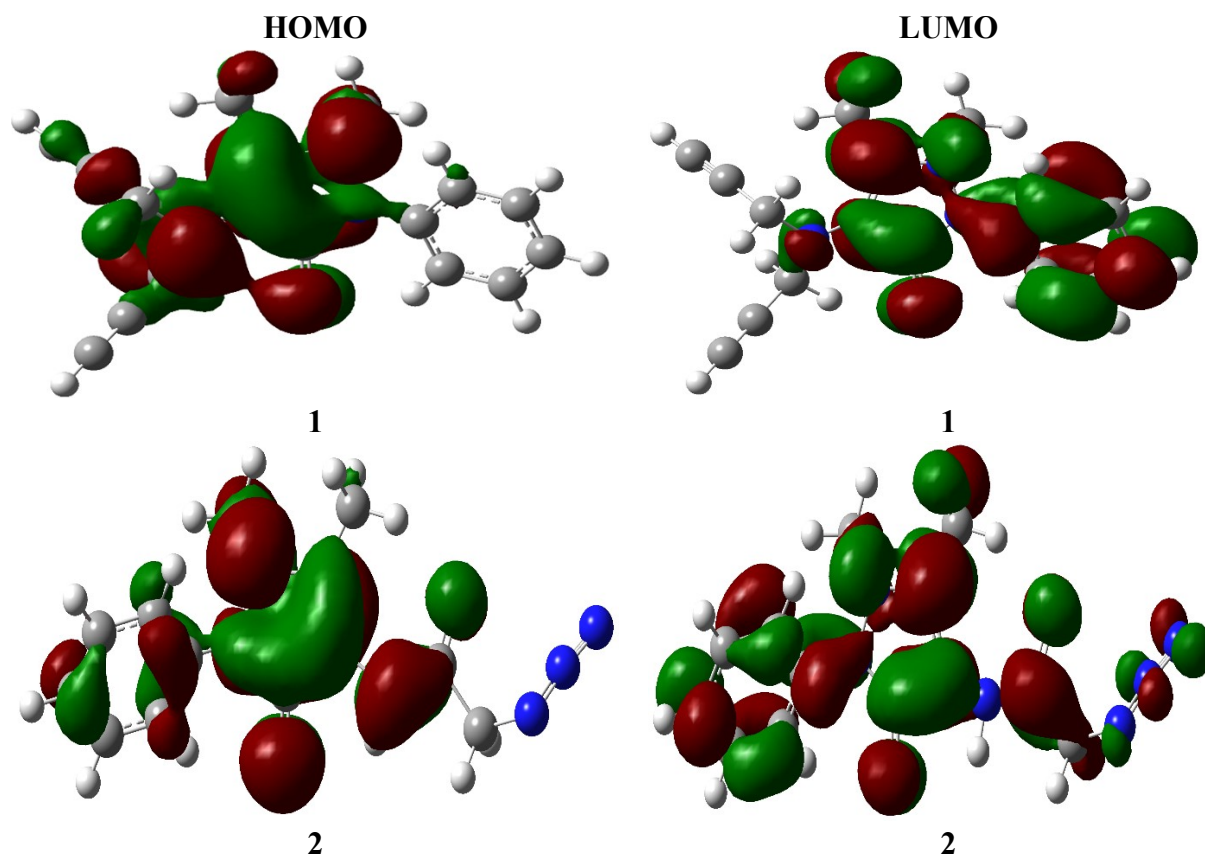


Figure SI-25. Optimized Structures of (a) APT.Cu²⁺ and (b) APT.Hg²⁺ Complexes

Table SI-2 Calculated FMOs, energy gap in eV at the B3LYP/6-311G(d,p) and B3LYP/LanL2DZ level of theory.

Sr. No.	Comp.	HOMO	LUMO	$\Delta E_{\text{LUMO-HOMO}}$
1.	1(Alkyne)	-5.41	-0.81	4.60
2.	2(Azide)	-6.09	-1.24	4.84
3.	APT	-5.31	-0.97	4.34
4.	APT.Cu ²⁺	-4.85	-1.30	3.56
5.	APT.Hg ²⁺	-4.07	-3.79	0.28



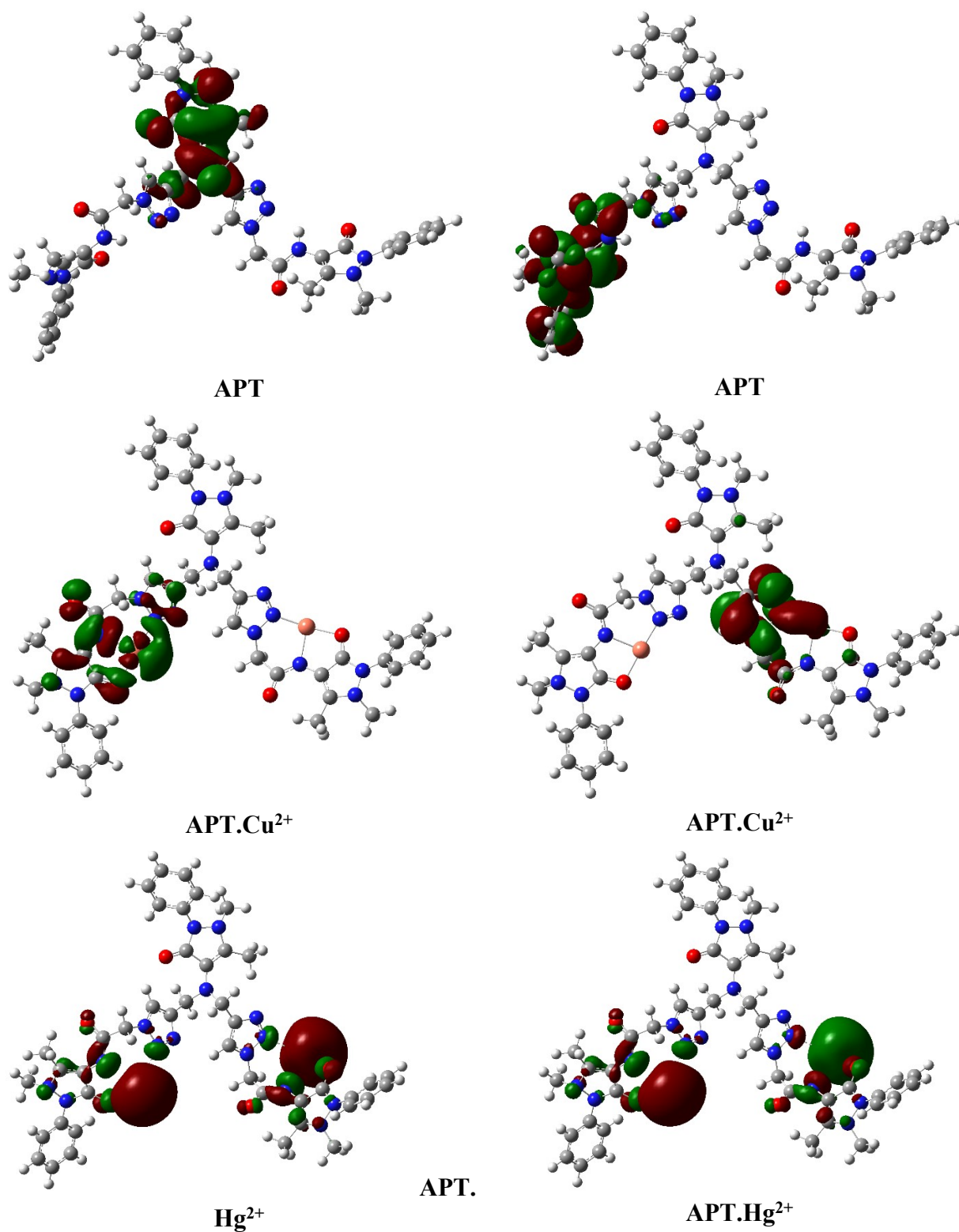


Figure SI-26. Highest occupied and lowest unoccupied molecular orbitals (HOMO and LUMO) distribution at the ground state of molecules **1**, **2**, APT, APT.Cu²⁺ and APT.Hg²⁺ complex

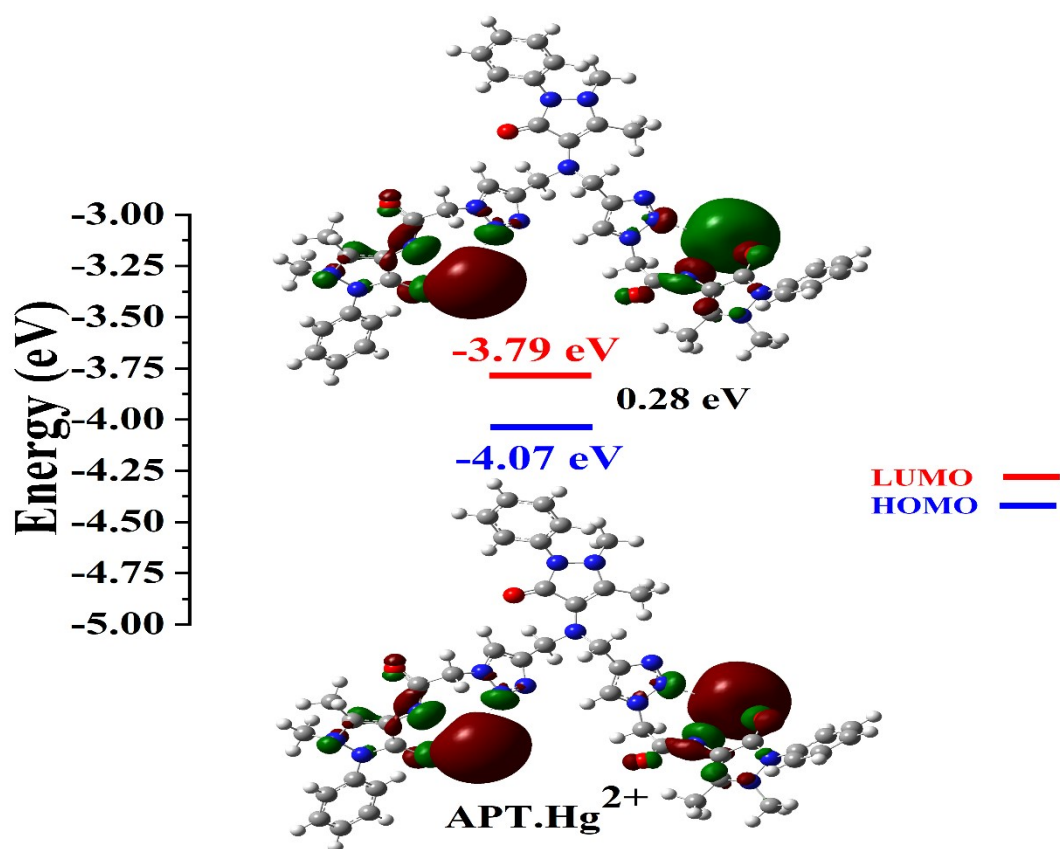


Figure SI-27. Contour plots of the frontier orbitals of the complex APT.Hg²⁺.

Reference:

- 1 G. M. Sheldrick, *Acta Crystallogr. Sect. C*, 2015, **71**, 3–8.
- 2 G. M. Sheldrick, *Acta Crystallogr. Sect. A*, 2015, **71**, 3–8.
- 3 O. V Dolomanov, L. J. Bourhis, R. J. Gildea, J. A. K. Howard and H. Puschmann, *J. Appl. Crystallogr.*, 2009, **42**, 339–341.
- 4 G. Singh, Suman, Diksha, Pawan, Mohit, Sushma, Priyanka, A. Saini and P. Satija, *J. Mol. Struct.*, 2022, **1250**, 131766.
- 5 S. Murtaza, A. A. Altaf, M. Hamayun, K. Iftikhar, M. N. Tahir, J. Tariq and K. Faiz, *Eur. J. Chem.*, 2019, **10**, 358–366.